Surface & Coatings Technology 337 (2018) 404–410

Contents lists available at ScienceDirect

Surface & Coatings Technology

journal homepage: www.elsevier.com/locate/surfcoat

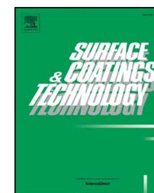

Phase-controlled growth of cobalt oxide thin films by atomic layer deposition

Soonyoung Jung[a], Dip K. Nandi[a], Seungmin Yeo[b], Hyungjun Kim[b], Yujin Jang[c], Jong-Seong Bae[c], Tae Eun Hong[c], Soo-Hyun Kim[a,*]

[a] School of Materials Science and Engineering, Yeungnam University, 214-1, Dae-dong, Gyeongsan-si 712-749, Republic of Korea
[b] School of Electrical and Electronic Engineering, Yonsei University, Seodaemun-gu, Seoul 120-749, Republic of Korea
[c] Busan Center, Korea Basic Science Institute, 1275 Jisadong, Gangseogu, Busan 618-230, Republic of Korea

ARTICLE INFO

Keywords:
Cobalt oxide
Atomic layer deposition
CoO
Co_3O_4
Optical bandgap

ABSTRACT

Cobalt oxide (CoO_x) thin films were deposited on thermally grown SiO_2 substrates by atomic layer deposition (ALD) using bis(1,4-di-iso-propyl-1,4-diazabutadiene)cobalt ($C_{16}H_{32}N_4Co$) and oxygen (O_2) as reactants at deposition temperatures ranging from 125 to 300 °C. X-ray diffraction (XRD) and Raman spectroscopic analysis indicated that a mixed-phase oxide consisting of CoO and Co_3O_4 was deposited at temperatures ranging from 125 to 250 °C. However, single-phase Co_3O_4 was deposited above the deposition temperature of 275 °C. Further, analyses by Rutherford backscattering spectrometry, transmission electron microscopy, and selected area electron diffraction along with XRD and Raman spectroscopy revealed that the single-phase cobalt oxide film was stoichiometric crystalline (spinel structure) with negligible N and C impurities. The optical band gap of the single-phase Co_3O_4 film was 1.98 eV and increased with decreasing deposition temperature. It was also shown that the mixed-phase cobalt oxide thin films could be converted into single-phase spinel Co_3O_4 by annealing at 350 °C in O_2 ambient. It was further observed that the phase of the ALD-grown cobalt oxide thin film could be controlled by controlling the precursor or reactant pulsing condition. The study revealed that pure Co_3O_4 phase could be grown at a relatively low temperature (250 °C) by using water vapor as a reactant. Therefore, this work systemically demonstrated several pathways to grow single-phase Co_3O_4 by ALD using a novel metalorganic cobalt precursor.

1. Introduction

Transition metal oxides have drawn considerable attention of the scientific community due to their abundance, non-toxicity, and chemical stability, as well as low-cost production methods [1]. Among the transition metal oxides, cobalt oxide (CoO_x) has been extensively studied for its potential use in various applications such as solid-state gas sensors [2], heterogeneous catalysts [3–5], resistance random access memory devices [6], solar absorbers [7], catalysts for oxidation of different volatile organic compounds [8], intercalation compounds for energy storage, and protective coatings on the interconnects of solid oxide fuel cells [9]. Cobalt oxides exist in two different stable phases: one is Co_3O_4, which is a mixed valence compound, $Co^{II}Co_2^{III}O_4$, with a normal spinel structure, and the other is the thermodynamically stable CoO, which is stable in a rock-salt structure at temperatures above 900 °C. However, the $Co^{II}O$ phase is known to be kinetically stable at room temperature. Along with thermodynamic stability, several other advantages render spinel Co_3O_4 preferable over rock-salt CoO. For example, spinel Co_3O_4 is beneficial as an intercalation host material in Li-ion batteries because of its large unit cell (0.808 nm) compared with that of rock-salt CoO (0.427 nm) and greater number of interstitial sites. As a result, Co_3O_4 exhibits a higher reversible capacity of 1100 mAh/g in Li-ion batteries compared with the 640 mAh/g capacity of CoO [10]. The other advantages of Co_3O_4 over the CoO phase include its relatively high electrochromic efficiency ($\approx 25\ cm^2/C$), large surface area, high conductivity, and better electrochemically stability [11].

Many kinds of thin film deposition techniques such as sputtering [12,13], reactive electron-beam evaporation [14], pulsed laser deposition (PLD) [15], spray pyrolysis [7,16–18], and chemical vapor deposition (CVD) [9,11,19–23] have been used for obtaining single-phase Co_3O_4 thin films. All these studies reported that single-phase Co_3O_4 thin films were difficult to prepare and could be obtained only in limited conditions of oxygen partial pressure and deposition temperature. For example, a previous work on CVD cobalt oxide [11] showed that single-

* Corresponding author.
E-mail address: soohyun@ynu.ac.kr (S.-H. Kim).

https://doi.org/10.1016/j.surfcoat.2018.01.047
Received 11 October 2017; Received in revised form 10 January 2018; Accepted 15 January 2018
Available online 19 January 2018
0257-8972/ © 2018 Elsevier B.V. All rights reserved.

phase Co_3O_4 was generally formed at relatively high O_2 flow rates, a high chamber pressure of 10 mbar, and high deposition temperatures above 450 °C. Moreover, even though the fabrication of single-phase Co_3O_4 is possible using physical vapor deposition (PVD)-based methods or CVD, these methods have an inherent limitation against application to potential high-performance devices with complex, small-sized, and high-aspect ratio structures.

Atomic layer deposition (ALD), as a thin film deposition technique, has attracted great interest due to its self-limiting nature of growth and exceptional coating conformality on three-dimensional structures with high aspect ratios. The self-limiting nature of ALD further provides the scope for monolayer growth as well as precise control over the film thickness over a large area. Cobalt oxide films have been prepared by ALD using an inorganic precursor such as cobalt diiodide (CoI_2) and O_2 [24]. Even though the resulting phase was single-phase Co_3O_4, the growth temperature was high, ranging from 475 to 600 °C. The deposition temperature could be decreased reasonably down to 100–400 °C using metalorganic cobalt precursors such as Co(II)-2,2,6,6-tetramethyl-3,5-heptanedionate [$Co(thd)_2$] [25] or bis(cyclopentadienyl) cobalt ($CoCp_2$) [26]. The single-phase Co_3O_4 was formed with these two Co precursors and highly reactive oxidants compared with O_2 such as O_3 and O_2 plasma. However, the growth rates were significantly low at around 0.02–0.05 nm/cycle. Moreover, $Co(thd)_2$ and $CoCp_2$ are solid at room temperature; thus, high sublimation temperatures are required to obtain sufficient vapor pressures of the precursors. Further, cobalt oxide films were grown by ALD using carbonyl-based cobalt metalorganic precursors such as dicobalt hexacarbonyl *tert*-butylacetylene [$Co_2(CO_6)(HCC(CH_3)_3)$, CCTBA] [27] or cyclopentadienylcobalt dicarbonyl [$CpCo(CO)_2$] [28] with O_3 at 50–150 °C. Relatively high growths per cycle (approximately 0.08–0.1 nm/cycle) were obtained; however, when CCTBA was used, the mixed-phase CoO_x was deposited. Recently, a ALD-CoO_x process at a very low temperature of 50 °C using a new carbonyl-based precursor such as dicobalt octacarbonyl [$Co_2(CO)_8$] and O_3 was reported; the results showed the formation of mixed-phase films of CoO and Co_3O_4 [29]. The above results indicate that the presence of the carbonyl (CO) ligand in the metal precursors might be the cause of such a low-temperature ALD growth of the CoO_x film. However, it was difficult to grow single-phase Co_3O_4 at low deposition temperatures by using these carbonyl-based precursors. Moreover, thermal decompositions of precursors such as CCTBA, CpCo $(CO)_2$, or $Co_2(CO)_8$ do not allow cobalt oxide films to be deposited by an ideal ALD process at high temperatures, restricting the growth of pure spinel Co_3O_4. Table 1 summarizes the ALD-CoO_x processes previously reported.

In this paper, we report the development of a new ALD-CoO_x process using a novel Co metalorganic precursor and O_2 as the reactant, which is relatively milder than O_3 or O_2 plasma. Several process parameters such as deposition temperature, precursor and reactant pulsing times, and post-annealing were carefully considered, and finally, controlled growth of high-quality single-phase Co_3O_4 was achieved.

Table 1
Summary of results of the ALD-CoO_x processes.

Precursor	Reactant	ALD window (°C)	Growth rate (nm/cycle)	Phase	Refs.
CoI_2	O_2	475–600	0.20	Co_3O_4	[24]
$Co(thd)_2$	O_3	114–307	0.02	Co_3O_4	[25]
$CoCp_2$	O_3	137–331	0.041–0.045	CoO, Co_3O_4	[26]
$CoCp_2$	O_2 plasma	100–400	0.05	Co_3O_4	[26]
CCTBA	O_3	68–138	~0.083 (@68 °C) 0.11 (@80 °C)	CoO, Co_3O_4	[27]
$CpCo(CO)_2$	O_3	50–150	0.08–0.11	Co_3O_4	[28]
$Co_2(CO)_8$	O_3	N/A	0.57	CoO, Co_3O_4	[29]

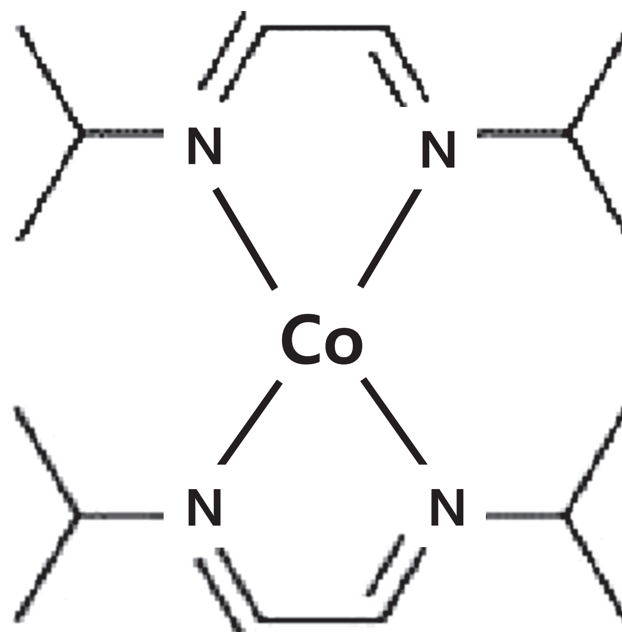

Fig. 1. Molecular structure of bis(1,4-di-iso-propyl-1,4-diazabutadiene)cobalt [$C_{16}H_{32}N_4Co$, $Co(dpdab)_2$] precursor.

2. Experiments

CoO_x films were deposited in a traveling-wave-type ALD reactor (Lucida-D100, NCD technology) using bis(1,4-di-iso-propyl-1,4-diazabutadiene)cobalt [$C_{16}H_{32}N_4Co$, $Co(dpdab)_2$] as the precursor and oxygen (O_2) or water vapor (H_2O) as the reactant (the typical reactant was O_2). The molecular structure of Co precursor is shown in Fig. 1. The Co precursor is liquid at room temperature and was heated to 95 °C during deposition, at which the vapor pressure was 0.25 Torr. The CoO_x films were deposited on p-type Si (100) wafers covered with a 100-nm-thick thermally grown SiO_2 layer and on glass substrates. The deposition temperature was varied from 125 to 300 °C, and the chamber pressure was fixed at approximately 0.5 Torr. The gas delivery line temperature was maintained at 105 °C to prevent condensation of the Co precursor during delivery. O_2 gas diluted with N_2 carrier gas was provided as a reactant into the chamber with a flow rate of 50 sccm. H_2O as a reactant was provided without a carrier gas. After each precursor and reactant pulsing step, a purging process was performed with 100 sccm of N_2. The basic pulsing conditions were set as follows: precursor pulsing for 10 s, reactant pulsing for 10 s, and purging for 10 s. These conditions were found to be sufficient to guarantee the self-limiting growth of the ALD-CoO_x films.

The properties of the CoO_x thin films were analyzed using various analytical techniques. The thicknesses of the CoO_x films were determined by X-ray reflectance (XRR, PANalytical X′-pert MRD with Cu-K_α radiation at 1.5 kW) and cross-sectional view scanning electron microscopy (XSEM, Hitachi S-4800, at 20 kV accelerating voltage and equipped with a field emission electron gun). For phase identification, grazing-incidence angle (incident angle, $\theta = 3°$) X-ray diffraction (GIAXRD) was performed. For precise phase identification, Raman spectroscopy was performed (HORIBA XploRA Plus with a 532-nm incident laser). Rutherford backscattering spectrometry (RBS) was performed to determine the film composition and possible incorporation of impurities in the film using He^{2+} with an incident energy of 2 MeV. Plan-view transmission electron microscopy (TEM, Tecnai F20, at 200 kV accelerating voltage and equipped with a field emission gun) was used to analyze the microstructures of the as-grown CoO_x films in

detail. The optical properties were analyzed by UV–Vis–NIR spectrophotometry (Cary 5000, Agilent Technologies). The as-grown mixed-phase CoO_x films were post-annealed in O_2 ambient using a RTA (rapid thermal annealing) system. The desired temperature for annealing could be reached within 10 s from room temperature using this RTA system. The post annealing process was carried out for 30 min at three different temperatures of 300, 350, and 400 °C.

3. Results and discussion

Prior to depositing the CoO_x films by ALD, the thermal stability of the metalorganic cobalt precursor was verified; this helped us set the reaction temperature within the ALD temperature window, avoiding decomposition-dominated growth of the film. For this test, only the Co precursor was pulsed into the chamber up to a temperature of 325 °C for 10 min, without introducing the counter-reactant, O_2. In this case, no film growth was observed, which indicates that the new Co precursor is thermally stable up to 325 °C, excluding the possibility of the growth by the thermal decomposition. Meanwhile, film deposition took place when O_2 vapor was pulsed after precursor pulsing (both for 10 s) at 275 °C, indicating that O_2 vapor was essential for growing ALD-CoO_x films in this study.

3.1. Effect of deposition temperature on the phase of ALD-CoOx thin films

The CoO_x films studied in this work were deposited under the self-limiting ALD growth condition, which has been described in the supporting information [Fig. 1(a) and (b) in Supporting information]. Fig. 2 shows the GIAXRD profiles of the ALD-CoO_x films deposited at temperatures ranging from 150 to 300 °C. The XRD results confirmed that the crystal structures of the ALD-grown CoO_x films obtained with deposition temperatures up to 250 °C had a mixed-phase consisting of CoO and Co_3O_4. However, single-phase Co_3O_4 was formed by increasing the deposition temperature to 265 °C and above. The XRD peaks of the mixed-phase CoO_x could be assigned to spinel Co_3O_4 [space group (no.): Fd3m (227) and lattice parameter (Å): a = 8.0837] and rock-salt CoO [space group (no.): Fm3m (225) and lattice parameter (Å): a = 4.2612]. The lattice planes were identified as (200) and (220) (at 2θ = 42.38° and 61.49°, respectively) (JCPDS no. 42–1719) of

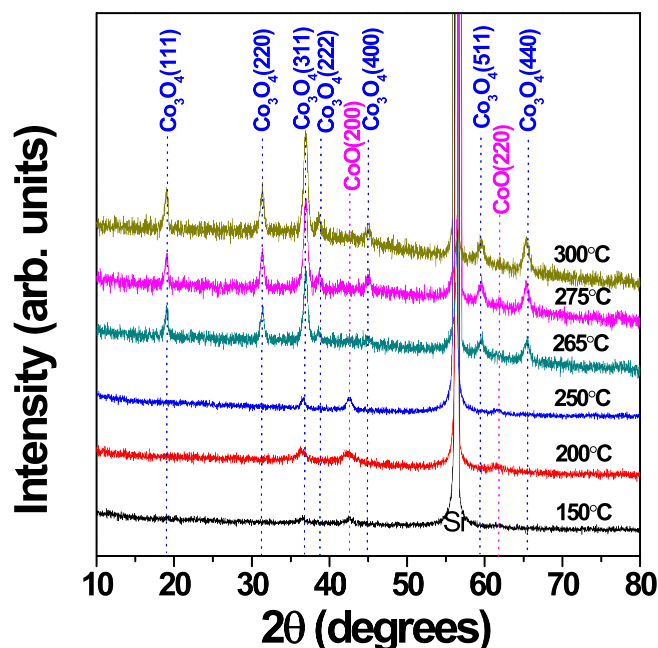

Fig. 2. XRD profiles of ALD-CoO_x films as a function of deposition temperature under basic pulsing conditions.

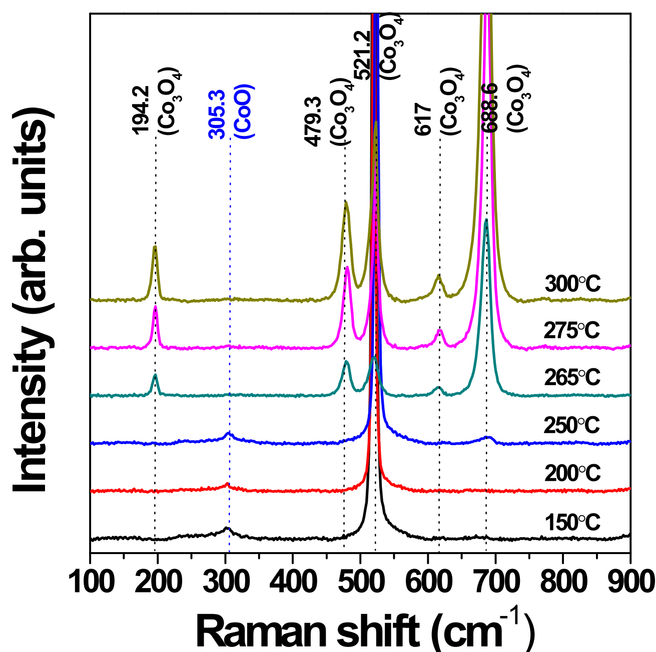

Fig. 3. Raman spectra of ALD-CoO_x films as a function of deposition temperature.

the rock-salt CoO and as (311) (2θ = 36.85°) (JCPDS no. 42–1467) of spinel Co_3O_4. It can be seen from Fig. 2 that the peaks corresponding to the (200) and (220) planes of CoO disappeared with increase in deposition temperature to 265 °C and above. On the contrary, several other peaks were observed in the XRD profile along with the (311) (2θ = 36.85°) peak of spinel Co_3O_4, which becomes more prominent with increasing deposition temperature. All these newly appeared XRD peaks at 2θ = 19.0001°, 31.27°, 38.54°, 44.81°, 59.36°, and 65.24° for the films deposited within the temperature range of 265–300 °C could be assigned to the (111), (220), (222), (400), (511) and (440) planes of spinel Co_3O_4, respectively. Interestingly, we did not observe any peak corresponding to rock-salt CoO at and above 265 °C. At the same time, all the peaks corresponding to the pure Co_3O_4 phase became more intense with increasing temperature, which reflects the better poly-crystallinity of the ALD-grown film. Thus, XRD analysis suggests that a sharp phase transformation from mixed-phase CoO_x to single-phase Co_3O_4 occurred at the deposition temperature of 265 °C and above.

To further confirm the phase change of ALD-CoO_x films deposited at different deposition temperatures, Raman spectroscopic analysis was performed in detail. Fig. 3 shows the Raman spectra of CoO_x films in the frequency range of 100–900 cm^{-1}. The Raman peaks of single-phase Co_3O_4 are well studied and are reported to appear at 194.2, 479.3, 521.2, 617, and 688.6 cm^{-1} [30]. The Raman peaks of CoO_x films deposited at temperatures ranging from 150 to 250 °C in this study were observed at around 305.3, 512.2, and 688.6 cm^{-1}. While the peaks at 521.2 and 688.6 cm^{-1} can be ascribed to the Raman-active modes of the Co_3O_4 phase, the peak observed at 305.3 cm^{-1} is assigned to CoO [31]. A close look at Fig. 3 reveals that the intensity of the peak at 305.3 cm^{-1} consistently decreases with increase in deposition temperature from 150 to 250 °C. Further observations showed that this peak completely disappeared for the films deposited at temperatures over 250 °C (265 to 300 °C). Therefore, the result confirms that the CoO_x films deposited within the temperature range of 150 to 250 °C have a mixed-phase comprising both CoO and Co_3O_4 phases. On the other hand, the Raman peaks of the CoO_x films deposited in the temperature range of 265 to 300 °C were observed at 194.2, 479.3, 521.2, 617, and 688.6 cm^{-1}. These five distinguished peaks could be identified as the Raman-active modes A_{1g} (688.6 cm^{-1}), E_g (479.3 cm^{-1}), and $3F_{2g}$ (194.2, 521.2, and 617 cm^{-1}) of Co_3O_4. Thus, Raman spectroscopic analysis provides complimentary information to XRD,

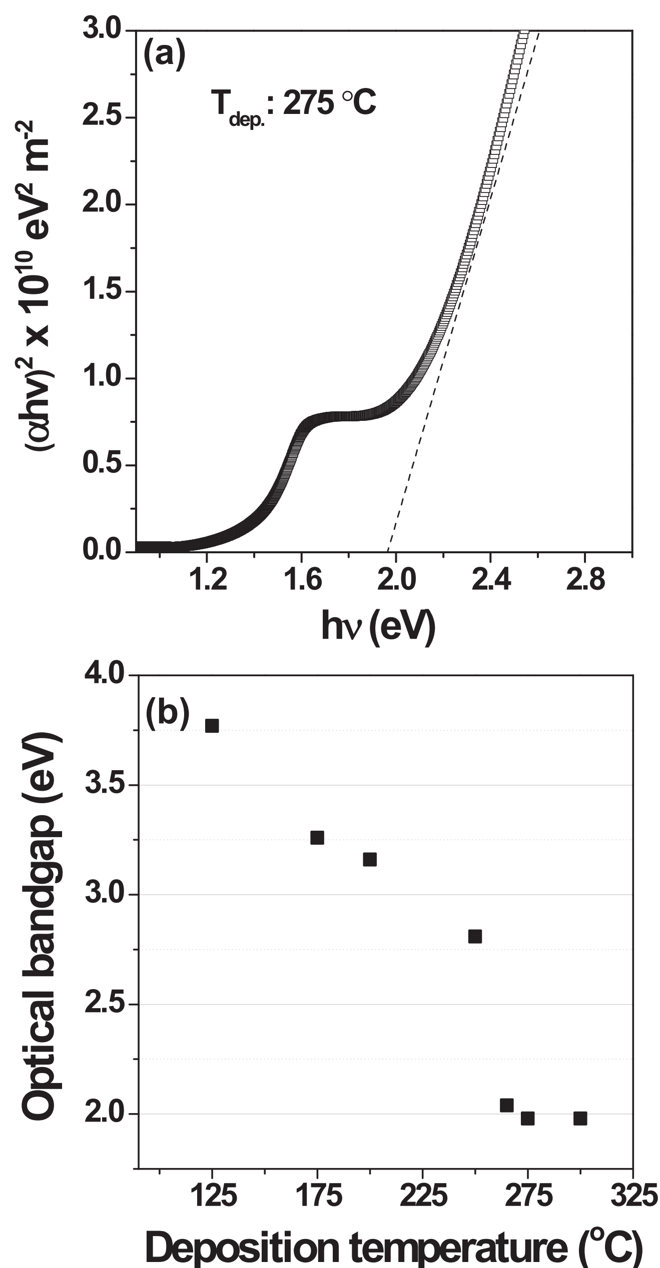

Fig. 4. Optical properties of ALD-CoO_x film deposited at 275 °C under basic pulsing condition: (a) plot of $(\alpha \cdot h\upsilon)^2$ as a function of photon energy and (b) optical band gap of ALD-CoO_x films as a function of deposition temperature.

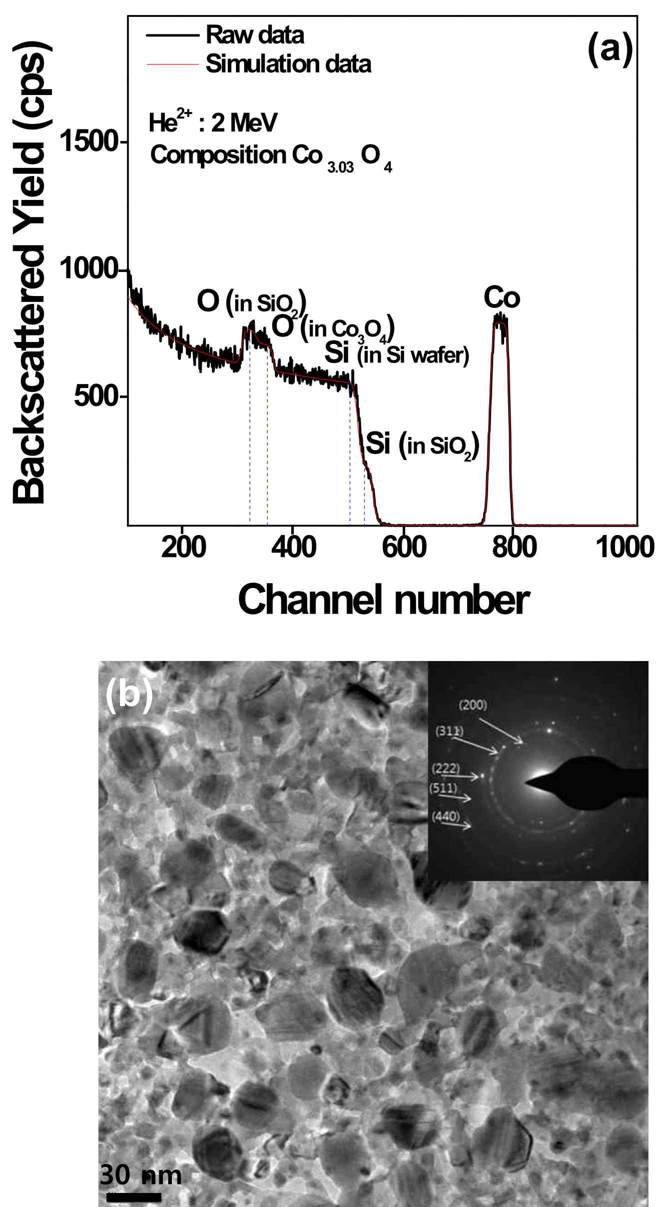

Fig. 5. (a) RBS spectra and (b) plan-view TEM bright-field (BF) image of as-grown ALD-Co_3O_4 film deposited at 275 °C. For RBS analysis, He^{2+} with incident energy of 2 MeV was used. Inset in (b): selected area electron diffraction pattern.

indicating a phase-controlled deposition of ALD-CoO_x that transformed from a mixed-phase oxide to single-phase Co_3O_4 depending on the deposition temperature.

Fig. 4(a) shows the representative optical property of the ALD-CoO_x film deposited at 275 °C, measured by UV–Vis–NIR spectrophotometry. The optical bandgap of the CoO_x films can be calculated from Eq. (1):

$$(\alpha \cdot h\upsilon)^n = A(h\upsilon - E_g), \quad (1)$$

where A is a constant, h is Planck's constant, n is the transition probability, α is the absorption coefficient of the material, ν is the frequency of the incident light, and E_g is the optical band gap. The optical bandgap was estimated by determining the intercept of the linear extrapolation with the photon energy for the absorption onset of the $(\alpha \cdot h\upsilon)^2$ curve. Fig. 4(b) shows the optical bandgaps of the ALD-CoO_x films at different deposition temperatures. The bandgaps of the CoO_x films generally decreased from 3.77 to 1.98 eV with increase in deposition temperature from 125 to 300 °C. However, interestingly, when the deposition temperature increased from 250 to 265 °C, a sharp decrease in optical bandgap from 2.8 to 2.0 eV was observed. With further increase in deposition temperature to 300 °C, the optical bandgap remained almost unchanged. This confirmed that phase transition from CoO and Co_3O_4 mixed-phase to single-phase Co_3O_4 occurred at the deposition temperature of 265 °C, which explains the sharp decrease in optical bandgap of the thin film deposited at 265 °C. In fact, it was reported that the optical bandgaps of single-phase Co_3O_4 thin films range from 1.48 to 2.2 eV [32], which is well matched with those of single-phase ALD-Co_3O_4 thin films in this study.

The above results clearly indicate that a single-phase Co_3O_4 film could be fabricated by controlling the deposition temperature. To further confirm the film composition and stoichiometry of the ALD-CoO_x film deposited at 275 °C, it was analyzed by RBS. Fig. 5(a) shows the RBS spectra of the ALD-CoO_x film (~100-nm-thick) on a SiO_2 (100-nm-thick)-coated Si wafer (400 μm in thickness). The He^{2+} ions backscattered from a collision with Co in the ALD-CoO_x films are shown at

channel numbers approximately ranging from ~740 to 800. A backscattering peak from Si consisted of two components. The peak appearing in the channel number range from ~550 to ~526 is the backscattered peak due the collision of He^{2+} with Si in the thermally grown SiO_2 and the peak appearing at a slightly lower channel number was from Si in the wafer. The backscattered peak from O also consisted of two components. The peak at the channel number of ~350 originated from O in the ALD-CoO_x films, while that at the channel number of ~300 arose from O in the SiO_2. Impurities such as carbon and nitrogen were not detected in RBS. Using RUMP simulation, the ratio of Co and O (Co/O) in the film was determined as 3.03:4, which supports the formation of a stoichiometric Co_3O_4 film. The sample was analyzed by plan-view TEM to confirm the phase and characterize the microstructure of the ALD-Co_3O_4 film in detail. The plan-view TEM bright-field (BF) images of the ALD-Co_3O_4 film deposited on SiO_2 (100 nm)/Si substrate showed that the film had a poly-crystalline structure [Fig. 5(b)] with irregular grain sizes. Its electron diffraction pattern [the inset in Fig. 5(b)] showed a typical concentric ring pattern with some clearly visible diffraction spots, which indicate that film had a poly-crystalline structure. The lattice fringes could be well assigned to the (200), (311), (222), (511) and (440) planes of cubic Co_3O_4. All these planes for single-phase Co_3O_4 were also evident in the XRD pattern of the ALD-CoO_x film grown at 275 °C. A careful view of the electron diffraction pattern reveals that the diffraction pattern is well matched with that of spinel Co_3O_4 but not with that of the CoO phase. From XRD and Raman analysis, it could be concluded that single-phase cubic Co_3O_4 could be deposited at a deposition temperature of 275 °C.

3.2. Effects of precursor and reactant pulsing conditions on the phase of ALD-CoO_x

This study further reveals that the phase of the ALD-grown CoO_x films could also be controlled by varying the precursor as well as reactant pulsing times, which are the key process parameters in ALD. It should be noted that deposition with the basic pulsing condition (precursor pulsing-purging-reactant pulsing-purging: 10 s each) resulted in the formation of a single-phase Co_3O_4 thin film at 275 °C. Fig. 6(a)(a) shows the XRD profiles of the films deposited at 275 °C by varying the precursor pulsing time with a fixed reactant pulsing time of 10 s. When the precursor pulsing time was increased from 1 to 10 s, the change in XRD peaks was not apparent though the intensities of the seven peaks appearing at $2\theta = 19°$, 31.27°, 36.85°, 38.54°, 44.81°, 59.36°, and 65.24° slightly increased. However, at a precursor pulsing time of 15 s, drastic changes in the XRD peaks were observed. The XRD peaks at $2\theta = 19.0001°$, 31.27°, 38.54°, 44.81°, 59.36°, and 65.24°, which could be attributed to spinel Co_3O_4 (111), (220), (222), (400), (511) and (440) planes, disappeared and the XRD peaks corresponding to rock-salt CoO appeared at $2\theta = 42.38°$ and 61.49°, indicating the formation of CoO phase. Fig. 6(b) shows the XRD profiles of the films prepared by varying the reactant pulsing time at a fixed precursor pulsing time of 10 s. When the reactant pulsing time was increased from 1 to 5 s, no change was observed in the positions of the XRD peak at $2\theta = 36.85°$, 42.38°, and 61.49° except a slight increase in the intensities of the peaks. The peaks at 42.38° and 61.49° could be as assigned to the (200) and (220) planes of rock-salt CoO, while the peak at 36.85° could be ascribed to the (311) plane of spinel Co_3O_4. However, when the reactant pulsing time was further increased to 7 s, changes in the XRD peaks were evident. The intensities of the XRD peaks at $2\theta = 42.38°$ and 61.49° arising from rock-salt CoO decreased and new XRD peaks corresponding to spinel Co_3O_4 appeared at $2\theta = 19°$, 31.27°, 38.54°, and 65.24° along with a peak at 36.85°, indicating the preferential formation of the Co_3O_4 phase. Further increasing the reactant pulsing time to 10 and 15 s led to a significant increase in the intensities of the XRD peaks at $2\theta = 19°$, 31.27°, 36.85°, 38.54°, 44.81°, 59.36° and 65.24°, reflecting the higher crystallinity of the Co_3O_4 phase. On the contrary, the peaks corresponding to the CoO phase completely

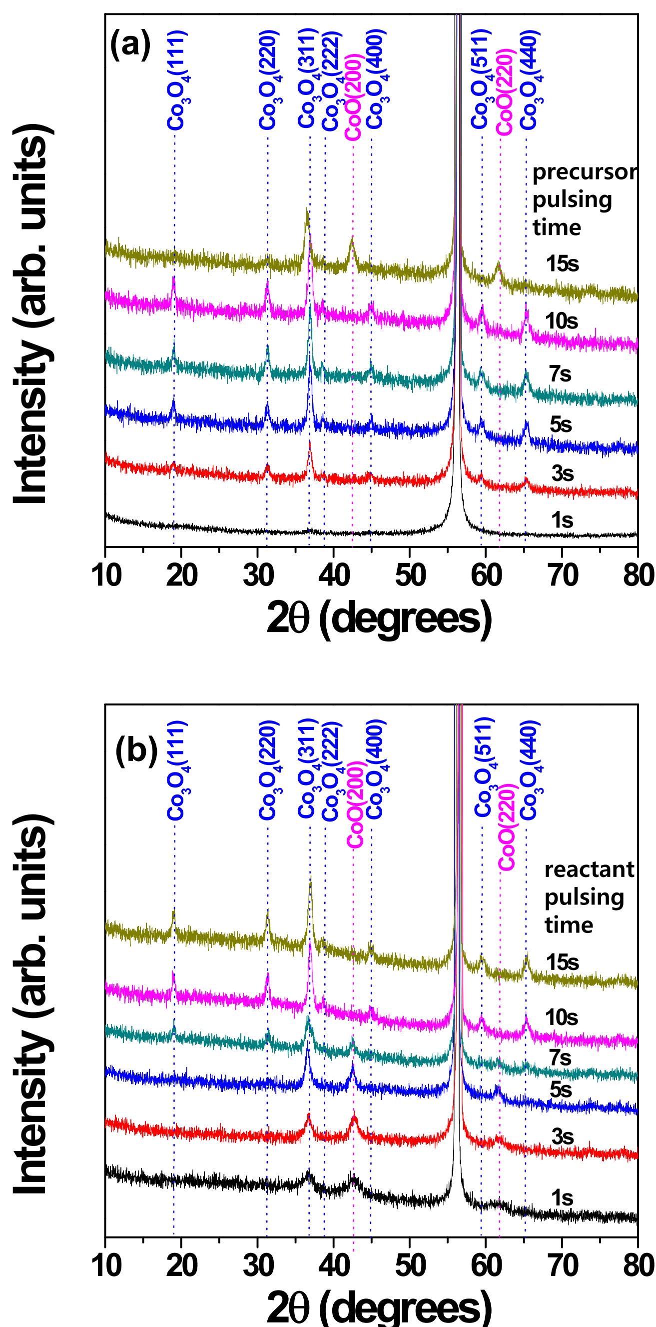

Fig. 6. XRD profiles of ALD-CoO_x films as a function of (a) precursor pulsing time and (b) reactant pulsing time at deposition temperature of 275 °C.

disappeared at these conditions of the reactant pulsing time. Thus, it could be concluded that an excess supply of Co metalorganic precursor with respect to the reactant (O_2) helped form the CoO phase as it has a higher Co to O ratio. On the other hand, an excess amount of reactant helped convert the phase from mixed CoO and Co_3O_4 to pure Co_3O_4.

3.3. Effect of post annealing in O_2 ambient on the phase of ALD-CoO_x

Post-annealing in O_2 ambient was performed to expand the process margin for obtaining single-phase Co_3O_4 films because the sharp transition from CoO and Co_3O_4 mixed-phase to single-phase Co_3O_4 occurred with a slight increase in the deposition temperature from 250 to 265 °C. Fig. 7(a) shows the XRD profiles of the CoO_x films annealed at different annealing temperatures. Here, the CoO_x films deposited at 250 °C with the basic pulsing condition were annealed in O_2 ambient at annealing

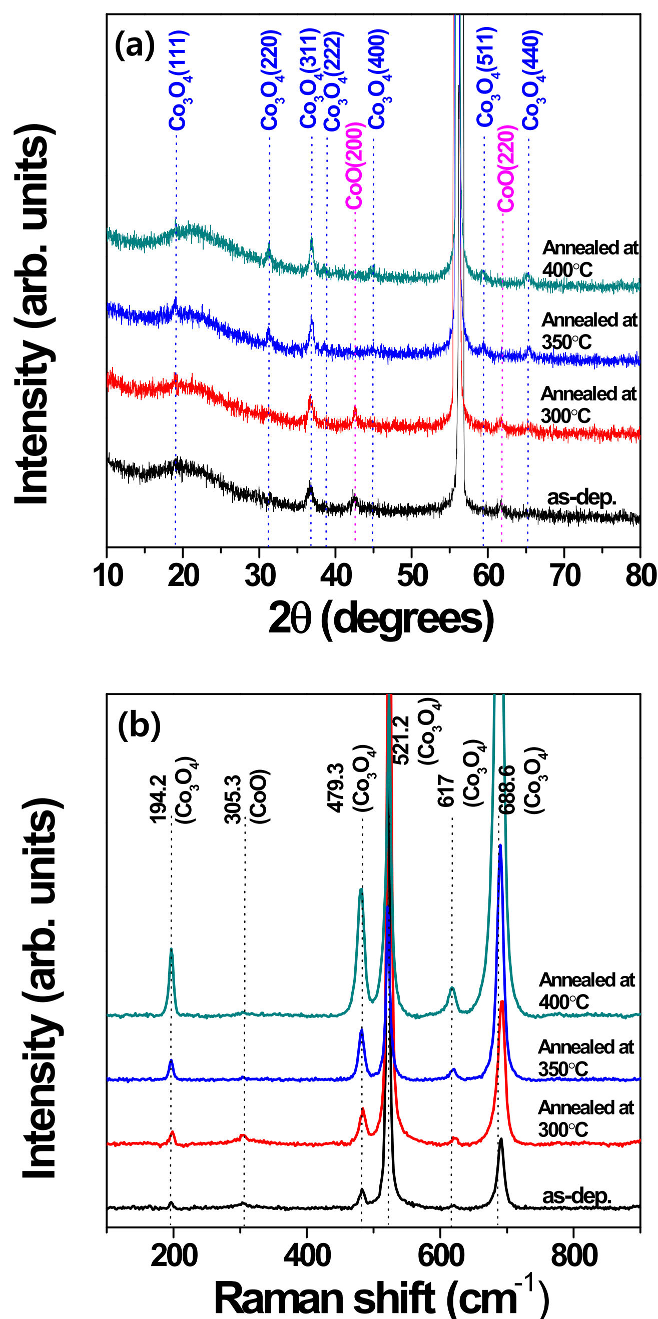

Fig. 7. (a) XRD profiles and (b) Raman spectra as a function of annealing temperature. The annealing temperature of the as-grown sample was 250 °C.

temperatures ranging from 300 to 400 °C for 30 min using the RTA process. The CoO_x films annealed at 300 °C had a mixed-phase with the formation of very small peaks at 2θ = 19.0001° and 31.27°, which were assigned to the (111) and (220) planes of cubic Co_3O_4. When the annealing temperature was increased to 350 °C, a change in the XRD profile was observed. Several new peaks appeared at 2θ = 19.0001°, 31.27°, and 59.36°, which could be attributed to the crystalline Co_3O_4 phase. On the contrary, the XRD peaks corresponding to (200) and (220) planes of rock-salt CoO disappeared completely. With further increase in annealing temperature to 400 °C, the peaks of Co_3O_4 became more intensified. This indicates an improvement in the crystallinity of cubic Co_3O_4 grains. Fig. 7(b) shows the Raman spectra, which complement the XRD results and confirm the phase change of the annealed CoO_x films with annealing temperature. Raman peaks were observed at 305.3, 521.2, and 688.6 cm^{-1} for the as-deposited CoO_x film ($T_{dep.}$: 250 °C). The peak at 305.3 cm^{-1} could be attributed to the CoO phase, while the other two peaks originated from Co_3O_4. Thus, it reveals the mixed-phase nature of the as-deposited film. In the case of sample annealed at 300 °C, two more Raman peaks appeared at 194.2 and 619 cm^{-1}, which were assigned to the Co_3O_4 phase, indicating the progressive formation of the Co_3O_4 phase. However, the peak at 305.3 cm^{-1} remained although its intensity decreased. Therefore, complete phase transformation from mixed-phase to single-phase Co_3O_4 did not occur at 300 °C; this was evident in the XRD analysis of the annealed film as well. However, when the annealing temperature was increased to 350 and 400 °C, the Raman-active mode for the CoO phase disappeared, confirming the formation of pure single-phase Co_3O_4. Similar to XRD, the peak intensities of all the five Raman-active modes corresponding to the Co_3O_4 phase increased with increasing annealing temperature, indicating the improvement in crystallinity of single-phase Co_3O_4 upon annealing.

3.4. ALD-CoO_x process using H_2O as a reactant

The above results showed that single-phase ALD-Co_3O_4 films could be controllably grown by controlling several process parameters such as the deposition temperature, precursor and reactant pulsing times, and the post-annealing process. We further tried to deposit single-phase ALD-Co_3O_4 films using another reactant, that is, water vapor. Fig. 8 shows the XRD profiles of the films grown using water vapor as a reactant at different deposition temperatures. The basic pulsing condition obtained for the ALD-CoO_x process with O_2 as a reactant (precursor pulsing-purging-reactant pulsing-purging: 10 s each) was used. For the ALD-CoO_x films deposited at temperatures ranging from 200 to 225 °C, the XRD peaks were well matched with those of rock-salt CoO (2θ = 42.38° and 61.49° for (200) and (220) planes, respectively) and spinel Co_3O_4 (2θ = 36.85° for (311) plane), indicating the formation of mixed-phase CoO_x. However, when the deposition temperature was increased to 250 °C and above, all the XRD peaks at 2θ = 19.0001°, 31.27°, 36.85°, 38.54°, 44.81°, 59.36°, and 65.24° could be perfectly assigned to the (111), (220), (311), (222), (400), (511), and (440) planes of single-phase spinel Co_3O_4, respectively. This result indicates that water vapor as a reactant during ALD growth can yield single-phase Co_3O_4 at a relatively low temperature. This implies that water

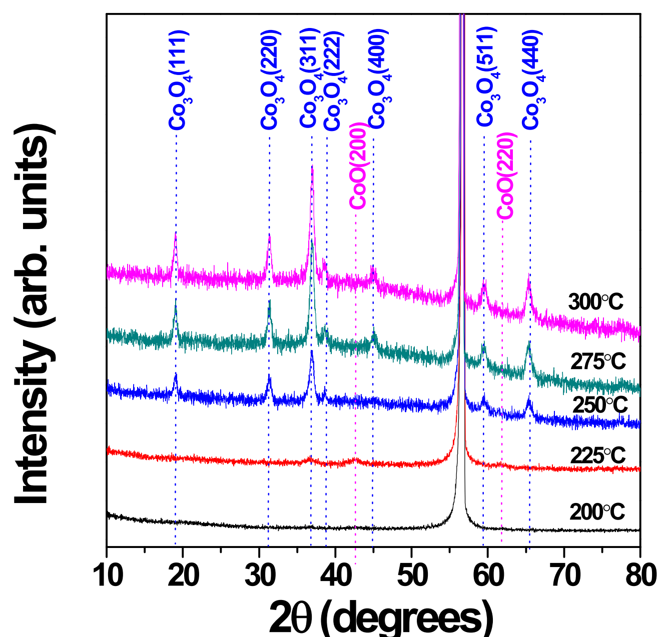

Fig. 8. XRD profiles of ALD-CoO_x films as a function of deposition temperature using water vapor as a reactant.

vapor acts as a strong oxidant compared with oxygen during the ALD of CoO_x using the present Co metalorganic precursor.

4. Summary and conclusions

In this study, CoO_x films were deposited on thermally grown SiO_2 and glass substrates by ALD with the sequential supply of $Co(dpdab)_2$ and O_2 at deposition temperatures ranging from 125 to 300 °C. CoO_x films deposited below 265°C were mixed-phase (rock-salt CoO and spinel Co_3O_4), as confirmed by XRD and Raman analysis. However, above 265 °C, single-phase Co_3O_4 films were successfully grown. The optical bandgaps of the ALD-CoO_x films varied with deposition temperature and decreased from 3.77 to 1.98 eV, indicating a change in the crystal structure of the films from mixed-phase to pure Co_3O_4 phase. RBS analysis confirmed that the single-phase film was quite stoichiometric (Co/O: 3.03:1) with negligible C and N impurities. This study confirms that the phase of the ALD-grown CoO_x thin film could also be controlled by controlling the precursor or reactant pulsing condition. Post-annealing at 350 °C in oxygen ambient also led to phase conversion from mixed-phase to single-phase Co_3O_4. Thus, this study systemically investigates the phase-controlled growth of ALD-CoO_x films by controlling several process parameters such as the deposition temperature, precursor and reactant pulsing times, and the post-annealing process. In addition, we could also fabricate single-phase Co_3O_4 films using water vapor as a reactant at deposition temperatures above 250 °C, which is slightly lower than that used for the ALD-CoO_x process with O_2 as a reactant. In conclusion, by controlling the various process parameters of ALD, it is possible to establish a process that can easily control the composition and phase of CoO_x films compared with other deposition processes, and can be applied to various applications.

Acknowledgements

This work was supported by Mid-career Researcher Program through the National Research Foundation of Korea (NRF) (2015R1A2A2A04004945), the Priority Research Centers Program through the NRF funded by the Ministry of Education (2014R1A6A1031189), and the MOTIE (Ministry of Trade, Industry & Energy (#10080651) and KSRC (Korea Semiconductor Research Consortium) support program for the development of the future semiconductor device. The precursor used in this study was provided by UP Chemical Co. Ltd., Korea.

Appendix A. Supplementary data

Supplementary data to this article can be found online at https://doi.org/10.1016/j.surfcoat.2018.01.047.

References

[1] R.F.P. Martins, A. Ahnood, N. Correia, L.M.N.P. Pereira, R. Barros, P.M.C.B. Barquinha, R. Costa, I.M.M. Ferreira, A. Nathan, E.E.M.C. Fortunato, Recyclable, flexible, low-power oxide electronics, Adv. Funct. Mater. 23 (2013) 2153–2161.

[2] H. Yamaura, J. Tamaki, K. Moriya, N. Miura, N. Yamazoe, Highly selective CO sensor using indium oxide doubly promoted by cobalt oxide and gold, J. Electrochem. Soc. 144 (1997) L158–L160.

[3] M. Haneda, Y. Kintaichi, N. Bion, H. Hamada, Alkali metal-doped cobalt oxide catalysts for NO decomposition, Appl. Catal. B Environ. 46 (2003) 473–482.

[4] D. Potoczna-Petru, L. Kępiński, Reduction study of Co_3O_4 model catalyst by electron microscopy, Catal. Lett. 73 (2001) 41–46.

[5] J.O. Chae, R. Pyagai, V. Demidiouk, S.I. Moon, D.Y. Lee, I.C. Choi, Influence of cobalt precursors on the catalytic activity of the cobalt oxide/Al_2O_3 catalysts, React. Kinet. Catal. Lett. 83 (2004) 369–375.

[6] H. Inoue, S. Yasuda, H. Akinaga, H. Takagi, Nonpolar resistance switching of metal/binary-transition-metal oxides/metal sandwiches: homogeneous/inhomogeneous transition of current distribution, Phys. Rev. B 77 (2008) 035105.

[7] A.G. Avila, E.C. Barrera, L.A. Huerta, S. Muhl, Cobalt oxide films for solar selective surfaces, obtained by spray pyrolysis, Sol. Energy Mater. Sol. Cells 82 (2004) 269–278.

[8] Z. Tian, N. Bahlawane, F. Qi, K. Kohse-Höinghaus, Catalytic oxidation of hydrocarbons over Co_3O_4 catalyst prepared by CVD, Catal. Commun. 11 (2009) 118–122.

[9] M. Burriel, G. Garcia, J. Santiso, A.N. Hansson, S. Linderoth, A. Figueras, Co_3O_4 protective coatings prepared by pulsed injection metal organic chemical vapor deposition, Thin Solid Films 473 (2005) 98–103.

[10] D. Larcher, G. Sudant, J.B. Leriche, Y. Chabre, J.M. Tarascon, The electrochemical reduction of Co_3O_4 in a lithium cell, J. Electrochem. Soc. 149 (2002) A234–A241.

[11] D. Barreca, C. Massignan, S. Daolio, M. Fabrizio, C. Piccirillo, L. Armelao, E. Tondello, Composition and microstructure of cobalt oxide thin films obtained from a novel cobalt (II) precursor by chemical vapor deposition, Chem. Mater. 13 (2001) 588–593.

[12] J.G. Cook, M.P. Van der Meer, The optical properties of sputtered Co_3O_4 films, Thin Solid Films 144 (1986) 165–176.

[13] H.K. Kim, T.Y. Seong, J.H. Lim, W.I. Cho, Y.S. Yoon, Electrochemical and structural properties of radio frequency sputtered cobalt oxide electrodes for thin-film supercapacitors, J. Power Sources 102 (2001) 167–171.

[14] J. Wöllenstein, M. Burgmair, G. Plescher, T. Sulima, J. Hildenbrand, H. Böttner, I. Eisele, Cobalt oxide based gas sensors on silicon substrate for operation at low temperatures, Sensors Actuators B Chem. 93 (2003) 442–448.

[15] R.J. Kennedy, The growth of iron oxide, nickel oxide and cobalt oxide thin films by laser ablation from metal targets, IEEE Trans. Magn. 31 (1995) 3829–3831.

[16] L.D. Kadam, P.S. Patil, Thickness-dependent properties of sprayed cobalt oxide thin films, Mater. Chem. Phys. 68 (2001) 225–232.

[17] P.S. Patil, L.D. Kadam, C.D. Lokhande, Preparation and characterization of spray pyrolysed cobalt oxide thin films, Thin Solid Films 272 (1996) 29–32.

[18] V.R. Shinde, S.B. Mahadik, T.P. Gujar, C.D. Lokhande, Supercapacitive cobalt oxide (Co_3O_4) thin films by spray pyrolysis, Appl. Surf. Sci. 252 (2006) 7487–7492.

[19] L.M. Apátiga, V.M. Castano, Magnetic behavior of cobalt oxide films prepared by pulsed liquid injection chemical vapor deposition from a metal-organic precursor, Thin Solid Films 496 (2006) 576–579.

[20] K. Shalini, A.U. Mane, S.A. Shivashankar, M. Rajeswari, S. Choopun, Epitaxial growth of Co_3O_4 films by low temperature, low pressure chemical vapour deposition, J. Cryst. Growth 231 (2001) 242–247.

[21] T. Maruyama, T. Nakai, Cobalt oxide thin films prepared by chemical vapor deposition from cobalt (II) acetate, Solar Energy Mater. 23 (1991) 25–29.

[22] D.G. Colombo, D.C. Gilmer, V.G. Young Jr, S.A. Campbell, W.L. Gladfelter, Anhydrous metal nitrates as volatile single source precursors for the CVD of metal oxide films, Chem. Vap. Depos. 4 (1998) 220–222.

[23] A.U. Mane, K. Shalini, A. Wohlfart, A. Devi, S.A. Shivashankar, Strongly oriented thin films of Co_3O_4 deposited on single-crystal MgO (100) by low-pressure, low-temperature MOCVD, J. Cryst. Growth 240 (2002) 157–163.

[24] M. Rooth, E. Lindahl, A. Hårsta, Atomic layer deposition of Co_3O_4 thin films using a CoI_2/O_2 precursor combination, Chem. Vap. Depos. 12 (2006) 209–213.

[25] K.B. Klepper, O. Nilsen, H. Fjellvåg, Growth of thin films of Co_3O_4 by atomic layer deposition, Thin Solid Films 515 (2007) 7772–7781.

[26] M. Diskus, O. Nilsen, H. Fjellvåg, Thin films of cobalt oxide deposited on high aspect ratio supports by atomic layer deposition, Chem. Vap. Depos. 17 (2011) 135–140.

[27] B. Han, K.H. Choi, K. Park, W.S. Han, W.J. Lee, Low-temperature atomic layer deposition of cobalt oxide thin films using dicobalt hexacarbonyl *tert*-butylacetylene and ozone, Electrochem. Solid-State Lett. 15 (2012) D14–D17.

[28] B. Han, K.H. Choi, J.M. Park, J.W. Park, J. Jung, W.J. Lee, Atomic layer deposition of cobalt oxide thin films using cyclopentadienylcobalt dicarbonyl and ozone at low temperatures, J. Vac. Sci. Technol. A 31 (2013) 01A145.

[29] D.K. Nandi, J. Manna, A. Dhara, P. Sharma, S.K. Sarkar, Atomic layer deposited cobalt oxide: an efficient catalyst for $NaBH_4$ hydrolysis, J. Vac. Sci. Technol. A 34 (2016) 01A115.

[30] J. Tyczkowski, R. Kapica, J. Łojewska, Thin cobalt oxide films for catalysis deposited by plasma-enhanced metal–organic chemical vapor deposition, Thin Solid Films 515 (2007) 6590–6595.

[31] B. Huang, K. Cao, X. Liu, L. Qian, B. Shan, R. Chen, Tuning the morphology and composition of ultrathin cobalt oxide films via atomic layer deposition, RSC Adv. 5 (2015) 71816–71823.

[32] A. Louardi, A. Rmili, T. Chtouki, B. Elidrissi, H. Erguig, A. El Bachiri, K. Ammous, H. Mejbri, Effect of annealing treatment on Co_3O_4 thin films properties prepared by spray pyrolysis, J. Mater. Environ. Sci. 8 (2) (2017) 485–493.